

Figure S1 *mahe* mRNA expresses in larval imaginal discs. Semi-quantitative RT PCR using *mahe* specific primer was performed to examine the expression of *mahe* in various larval tissues. *mahe* transcripts were present in RNA extracted from larval brain, eye-antennal disc, wing disc, fat body, salivary gland and leg discs. *rps17* was used as internal control and No RT (in the absence of reverse transcriptase) was done for each sample to rule out genomic DNA contamination.

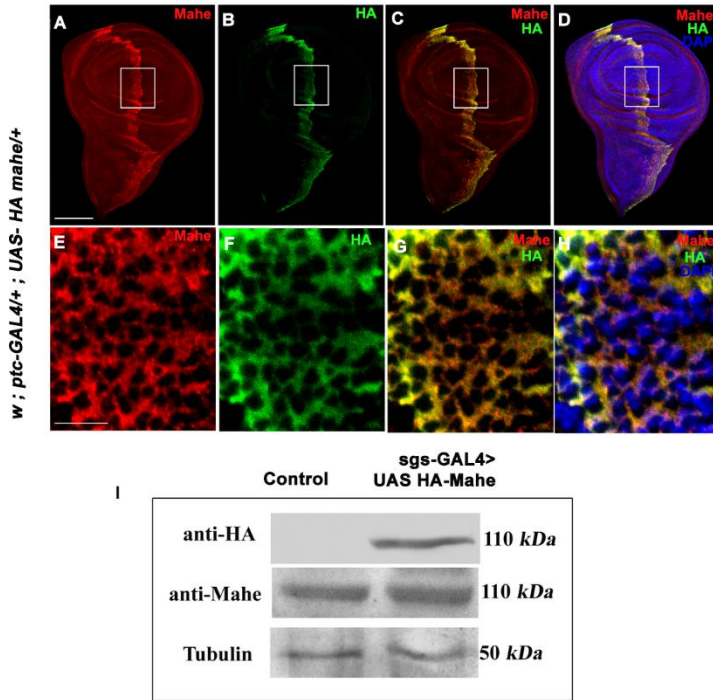


Figure S2 Detection of ectopic HA-Mahe in the wing imaginal disc. Immunostaining and western blotting was carried out with anti-Mahe and anti-HA antibody. (A-H) Over expressed HA-Mahe protein was localized throughout the cytoplasm and excluded from the nucleus as detected with anti-Mahe (Red, A and E) as well as anti-HA (Green, B and F) in wing imaginal discs. Lower panel is magnified view of boxed area from the upper panel. Western blot with both anti-Mahe and anti-HA detected a 110 kDa band from protein extract of *sgs-GAL4* salivary gland and *sgs-GAL4* driven UAS-HA Mahe salivary gland. Tubulin was used as loading control. Scale bar A-D is 100 μ m each and E-H is 10 μ m each.

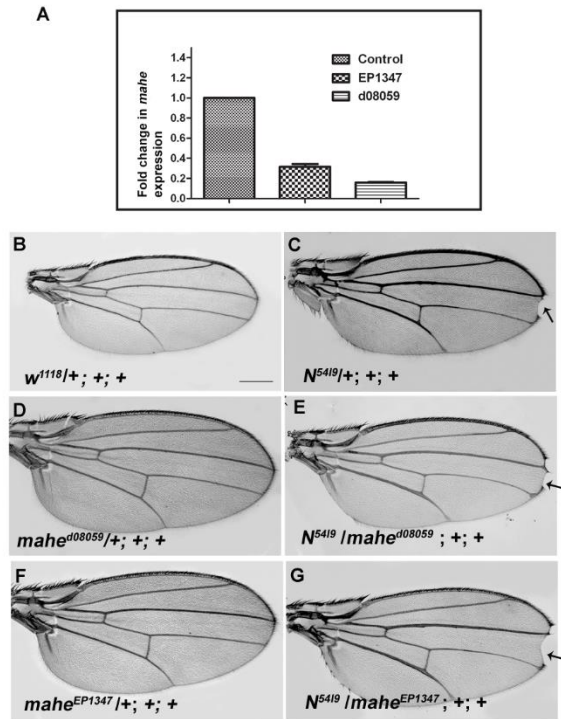


Figure S3. Genetic interaction of *mahe*^{d08059} and *mahe*^{EP1347} hypomorphic alleles of *mahe* with *N*⁵⁴¹⁹ (Notch loss-of-function) allele. (A) RNA was extracted from five days old adult flies and real time PCR was performed with *mahe* specific primers to monitor *mahe* transcript level in P element insertion (P{XP} d08059 (*mahe*^{d08059}) and EP1347 (*mahe*^{EP1347}) lines, *mahe* transcripts were significantly lowered in these two P element insertion lines when compared to that of control. (B) Wing with normal morphology. (C) Heterozygous Notch allele *N*⁵⁴¹⁹/+ shows mild notching at the wing margin. (D) Heterozygous *mahe* allele (*mahe*^{d08059}) shows normal wing morphology. (E) Trans-heterozygous combination of *N*⁵⁴¹⁹ and *mahe*^{d08059} results in enhancement in wing notching phenotype. (F) Heterozygous *mahe* allele (*mahe*^{EP1347}) shows normal wing morphology. (G) Trans-heterozygous combination of *N*⁵⁴¹⁹ and *mahe*^{EP1347} also results in enhancement in wing Notching phenotype. Scale bar B-G, 200 μ m each.

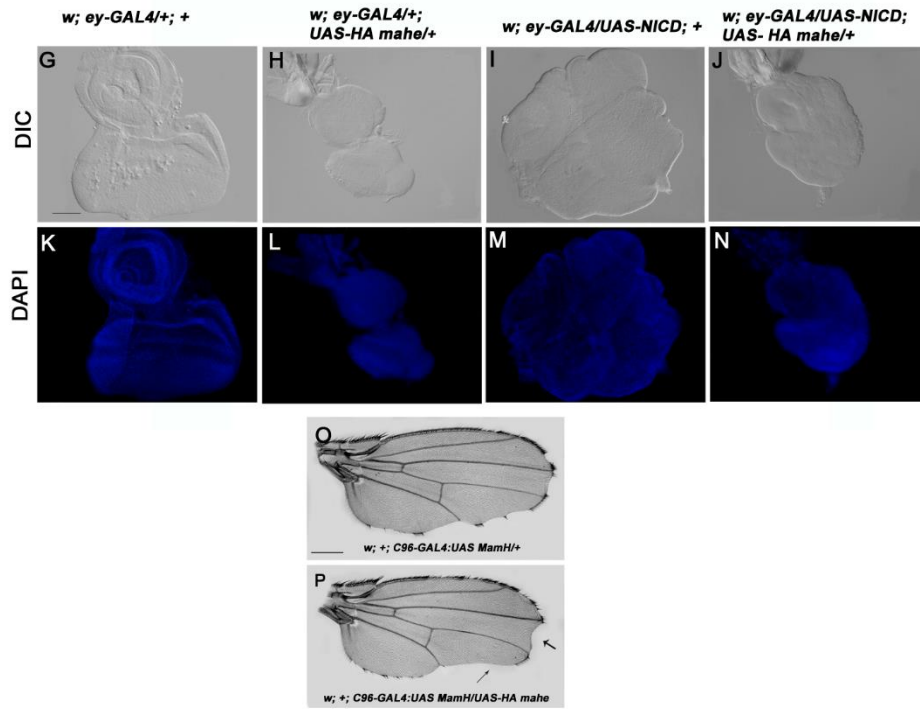


Figure S4 Genetic interaction of *mahe* with Notch gain-of-function background. (A) Eye-antennal disc with normal morphology. (B) *ey-GAL4* driven expression of *mahe* results in massive reduction in size of eye-antennal disc. (C) *ey-GAL4* driven expression of activated form of Notch (NICD) results in dramatic proliferation of eye tissue. (D) Co-expression of Mahe and NICD with *ey-GAL4* results in significant rescue of Notch mediated proliferation in eye antennal disc. (E) Dominant negative form of *Mam* driven with *C96-GAL4* results in nicked wing margin. (F) In combination with over expressed *mahe*, this phenotype was moderately enhanced (arrow). Scale bar A-H is 50 μ m each and I, J is 200 μ m each.

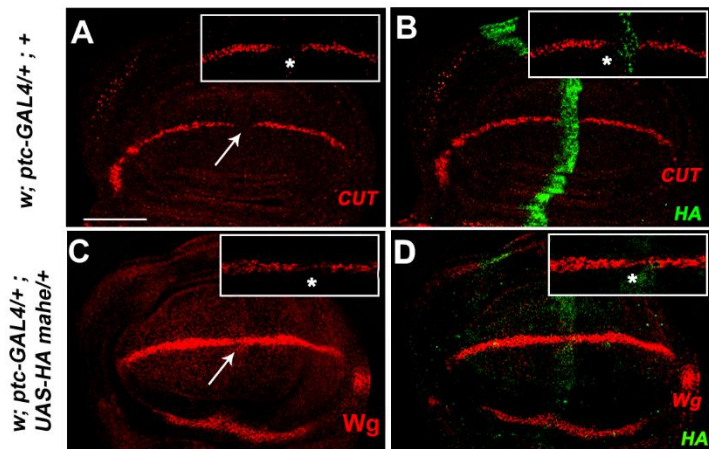


Figure S5 Ectopic-HA Mahe inhibits Notch signalling. (A-D) Ectopic expression of HA Mahe results in loss of Cut and Wg staining (arrow). (B, D) Double staining of HA, Cut (B) and HA, Wg (D) shows that loss of Cut and Wg expression was specific to *mahe* over expression domain. Scale bar A-D is 50µm each.